

Quarkonium polarization in low- p_T hadro-production: from past data to future opportunities

Pietro Faccioli¹⁾, Ilse Krätschmer²⁾ and Carlos Lourenço³⁾

Abstract

Several fixed-target experiments reported J/ψ and Υ polarization measurements, as functions of Feynman x (x_F) and transverse momentum (p_T), in three different polarization frames, using different combinations of beam particles, target nuclei and collision energies. The data form such a diverse and heterogeneous picture that, at first sight, no clear trends can be observed. A more detailed look, however, allows us to discern qualitative physical patterns that inspire and support a simple interpretation: the directly-produced quarkonia result from either gluon-gluon fusion or from quark-antiquark annihilation, with the former mesons being fully longitudinally polarized and the latter being fully transversely polarized. This hypothesis provides a reasonable quantitative description of the J/ψ and $\Upsilon(1S)$ polarizations measured in the $x_F \lesssim 0.5$ kinematical domain. We provide predictions that can be experimentally tested, using proton and/or pion beams, and show that improved J/ψ and $\psi(2S)$ polarization measurements in pion-nucleus collisions can provide significant constraints on the poorly known parton distribution functions of the pion.

arXiv:2210.09845v1 [hep-ph] 18 Oct 2022

¹⁾ LIP, Lisbon, Portugal, Pietro.Faccioli@cern.ch

²⁾ ISTA, Klosterneuburg, Austria, Ilse.Kraetschmer@gmx.at

³⁾ CERN, Geneva, Switzerland, Carlos.Lourenco@cern.ch

1 Introduction

Charmonium and bottomonium production provides an ideal case study for the understanding of hadron formation in quantum chromodynamics (QCD) [1]. Its theoretical description is based on the generally agreed assumption that the charm and beauty quarks (the heaviest ones capable of forming bound states) are heavy enough to allow the factorization of short- and long-distance effects. Within the non-relativistic QCD (NRQCD) framework [2], in particular, perturbative QCD computations provide the production cross sections of the $Q\bar{Q}$ pre-resonance (the “short-distance coefficients”, SDCs), while the non-perturbative evolution of the $Q\bar{Q}$ state to the observed meson (the hadronization step) is described by phenomenological parameters (the “long-distance matrix elements”, LDMEs), determined from fits to experimental data. Other theoretical approaches have been considered, such as the colour-singlet model (CSM) [3,4] and the colour-evaporation model (CEM) [5,6]. These theoretical models differ in the choice and classification of the allowed pre-resonance configurations. The NRQCD approach foresees the contribution of all possible spin, S , orbital angular momentum, L , total angular momentum, J , and colour ($c = 1, 8$) configurations, $Q\bar{Q}(^{2S+1}L_J^{[c]})$, organized in an expansion in powers of the relative $Q\bar{Q}$ velocity, $v < 1$, so that only a small number of leading and sub-leading terms remain quantitatively important. Instead, the CSM considers that the final-state hadron can only result from a colour-neutral (singlet) pre-resonance having the same quantum numbers and the CEM is built upon the assumption that one universal hadronization factor per quarkonium state (independent of the S, L, J configuration) multiplies the short-distance $Q\bar{Q}$ production cross section.

The fundamental question that all models address is: how are the observable kinematic properties of the produced quarkonium meson related to the quantum state of the unobservable $Q\bar{Q}$ pre-resonance? The answers are different because, among other factors, the several contributing short-distance processes are scaled by different long-distance weights. The observable *polarization* of the quarkonium state provides particularly significant information regarding the hadronization model, given that it directly reflects the mixture of S, L, J configurations (and polarizations) of the contributing pre-resonance states. The polarizations of five vector quarkonia (J/ψ , $\psi(2S)$, $\Upsilon(1S)$, $\Upsilon(2S)$ and $\Upsilon(3S)$) have recently been measured at relatively high transverse momentum, p_T , both at the Tevatron [7] and at the LHC [8–12]. These measurements, showing no significant signs of polarization, have been addressed in many studies, including analyses based on the NRQCD [13–20] and CEM [21] approaches.

In this paper we devote our attention to low- p_T quarkonium hadro-production, a kinematical domain complementary to that explored at the LHC. We start by considering the polarization measurements reported by several fixed-target experiments, at CERN, DESY and Fermilab, using proton or pion beams, in a broad energy range, colliding on targets made of several materials. The question we address here is: can this multitude of low- p_T quarkonium polarization measurements be interpreted in a consistent physical picture? At first sight, we may think that it is very challenging to see coherent patterns emerging from a collection of results obtained in such a diverse set of kinematical conditions, affected by several difficulties in the detection and analysis techniques, and reported using three different polarization frames. Nevertheless, a careful look at the experimental results allows us to see that, while most data points fluctuate around the unpolarized condition, there are some tendencies towards strong polarizations in certain kinematical regions. These qualitative patterns motivate us to consider a simple physical interpretation of low- p_T quarkonium production, as a superposition of two 2-to-1 processes: gluon-gluon fusion

and quark-antiquark annihilation, respectively leading to the production of fully longitudinally polarized and fully transversely polarized mesons. Our study is exclusively focused on the polarization data and deliberately follows a model-independent approach. Reports on theoretical studies of low- p_T quarkonium cross sections can be found, for example, in Refs. [22–28].

The paper is structured as follows. Section 2 presents and reviews the experimental measurements we have considered. Section 3 discusses possible qualitative indications from the peculiar data patterns, which are then developed in Section 4 into a simple model. Quantitative comparisons between the model and the experimental measurements are shown in Sections 5 and 6, while predictions for future experiments are provided in Section 7.

2 Experimental data

Figures 1 and 2 present, respectively for the J/ψ and Υ states, polarization measurements made by fixed-target experiments, listed in Table 1, using proton or pion beams and several target materials. The considered observable, shown as functions of x_F and p_T , is the polar anisotropy parameter λ_ϑ [29]. Most of the measurements address J/ψ production [30–41], with only one measurement of Υ production [42]. The ensemble of experiments covers an overall kinematical domain defined by $-0.3 \lesssim x_F \lesssim 1$ and $0 < p_T \lesssim 5$ GeV, with average p_T between 1.0 and 1.2 GeV and average p_T squared in the $1.5 \lesssim \langle p_T^2 \rangle \lesssim 2.2$ GeV² range.

The polarizations were measured in three different frames: Collins–Soper (CS) [43], Gottfried–Jackson (GJ) [44] and centre-of-mass helicity (HX), where the polarization axis z is defined, respectively, as the relative direction of the colliding nucleons, the direction of one of the two nucleons (generally the beam proton), and the direction of the quarkonium itself with respect to the centre-of-mass of the system of the two nucleons.

Since each of the several experiments that measured the polarization of J/ψ mesons used different combinations of beam particles, target nuclei and collision energy, it is, a priori, not surprising to see that the six panels of Fig. 1 display a rather scattered overall picture. The collision energies span a broad range, from $\sqrt{s} = 15.3$ to 41.6 GeV, while the target nuclei include eight elements between hydrogen and tungsten. The beam particles include pions (both charges), protons and antiprotons, and even indium nuclei. And in the case of secondary beams (e.g., the pion and antiproton cases), the beam composition is contaminated by some fraction of other particles, which adds further complexity to the picture. These complications can be illustrated with a few examples. E444 collected data with a beam composed of several particles (π^\pm , K^\pm , p, \bar{p}) hitting a target system composed of several materials (C, Cu, W), the combination π^- -C being the most important. WA11 collected 40% of the data at 140 GeV beam momentum and 60% at 150 GeV. E537 collected data with several beam-target configurations; the J/ψ sample is dominated by the π^- -W combination but there is also an important contribution (around 25% of the events) from \bar{p} -W collisions, while the data collected with Be and Cu targets, with both beams, is a negligible contamination.

Besides the diversity of collision energies, beam particles and target nuclei, which surely contributes to the visible spread of the data points, we also need to take into consideration that polarization measurements are always very challenging and it is quite possible that some of the reported systematic uncertainties are underestimated (in fact, some of the older results were even published without mentioning systematic uncertainties). In particular, most of the measurements were obtained from one-dimensional analyses, only considering

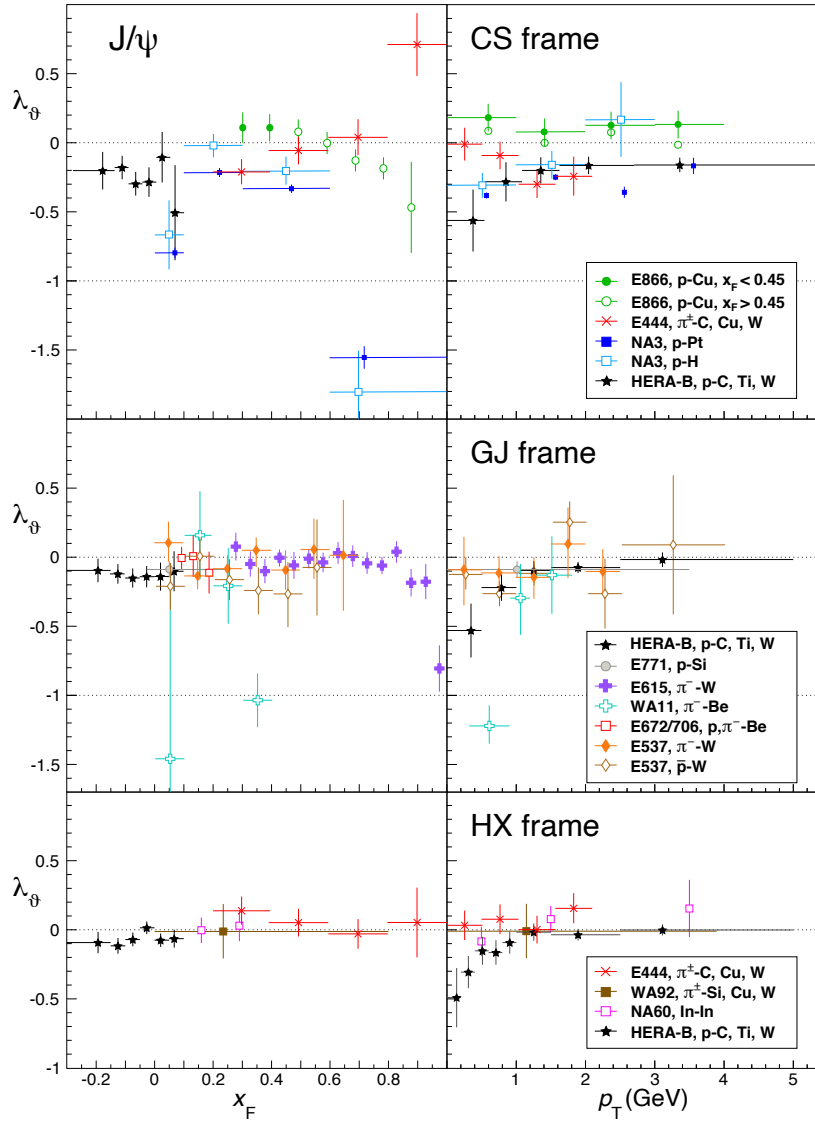


Figure 1: The J/ψ polar anisotropy parameter λ_θ measured in the CS, GJ, and HX frames (top to bottom), vs. x_F and p_T .

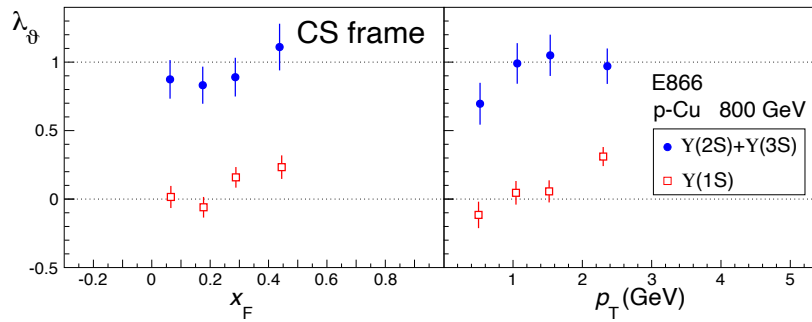


Figure 2: The $\Upsilon(1S)$ and $\Upsilon(2S+3S)$ polar anisotropy parameter λ_θ measured by E866 in the CS frame, vs. x_F and p_T .

Table 1: J/ψ and Υ polarization measurements in fixed target experiments, characterized by several beam energies (E_{lab}) and angular coverages, denoted using x_{F} , centre-of-mass rapidity (y_{cms}) or fractional momentum of the beam partons (x_1).

Exp. [Ref.]	Beam	Target	E_{lab} (GeV)	\sqrt{s} (GeV)	Δx_{F}	Δp_{T} (GeV)	$\langle p_{\text{T}} \rangle, \langle p_{\text{T}}^2 \rangle$ (GeV), (GeV ²)
J/ψ							
E537 [30]	π^- , \bar{p}	W	125	15.3	0.0–0.7	0–2.5	$\langle p_{\text{T}} \rangle = 1.04$
WA11 [31]	π^-	Be	146	16.6	0.0–0.4	0–2.4	$\langle p_{\text{T}} \rangle = 1.0$
NA60 [32]	In	In	158	17.2	$y_{\text{cms}}: 0-1$	$\approx 0-4$	
E444 [33]	π^\pm	C, Cu, W	225	20.6	$x_1: 0.2-1.0$	0–2.5	$\langle p_{\text{T}} \rangle = 1.2$
E615 [34]	π^\pm	W	252	21.8	0.25–1.0	0–5	
NA3 [35]	π^-	H, Pt	280	22.9	0.0–1.0		$\langle p_{\text{T}}^2 \rangle = 1.52, 1.85$
WA92 [36]	π^-	Si, Cu, W	350	25.6	$\approx 0.0-0.8$	0–4	
E672/706 [37]	π^-	Be	515	31.1	0.1–0.8	0–3.5	$\langle p_{\text{T}} \rangle = 1.17$
E672/706 [38]	p	Be	530, 800	31.5, 38.8	0.0–0.6		$\langle p_{\text{T}} \rangle = 1.15, 1.22$
E771 [39]	p	Si	800	38.8	–0.05–0.25	0–3.5	$\langle p_{\text{T}}^2 \rangle = 1.96$
E866 [40]	p	Cu	800	38.8	$\approx 0.0-0.5$	$\approx 0-4$	
HERA-B [41]	p	C, Ti, W	920	41.6	–0.34–0.14	0–5.4	$\langle p_{\text{T}}^2 \rangle = 2.2$
Υ							
E866 [42]	p	Cu	800	38.8	0.0–0.6	0–4	$\langle p_{\text{T}} \rangle = 1.3$

the $\cos\vartheta$ observable and neglecting acceptance correlations between the $\cos\vartheta$ and φ variables of the dilepton angular distribution, a practice that can easily lead to significantly biased results, as discussed in Refs. [29,45]. This might explain why some of the data points shown in Fig. 1 are outside of the physically allowed range (with $\lambda_\vartheta < -1$).

Despite the first impression that the diversity of points form a rather scattered overall picture, we can see that most of the J/ψ values fluctuate around the $\lambda_\vartheta = 0$ limit (unpolarized production), with some trends towards strong polarizations in certain points of the kinematic domain. Among all the J/ψ measurements, the one published by HERA-B [41] stands out as the only one that considers all three polarization frames (CS, GJ and HX) and that, furthermore, includes all three shape parameters of the angular distribution relevant for parity-conserving decays, λ_ϑ , λ_φ and $\lambda_{\vartheta\varphi}$ [29]. It will, therefore, provide a very useful beacon to guide our extraction of physically relevant trends (presented in the next section) from the seemingly cryptic data collection depicted in Fig. 1.

The most salient feature that one can easily see as standing out of the global picture is the polarization measurement reported by E866 for the (unresolved) $\Upsilon(2\text{S})$ plus $\Upsilon(3\text{S})$ states [42]. While the values reported for the $\Upsilon(1\text{S})$ mesons produced with $x_{\text{F}} < 0.45$ cluster around $\lambda_\vartheta \sim 0.1$ and are consistent with the J/ψ values provided by the same experiment, for identical experimental conditions [40], those reported for the 2S+3S states are surprisingly different: $\lambda_\vartheta \sim +1$. If we exclude the possibility of problems with the experimental measurement, this observation reveals an astounding difference between the polarizations observed for the excited states and for the ground state. Given that these three S-wave states are expected to have identical polarizations when directly produced (or

when being produced in decays of heavier S-wave states [46–48]), the observed difference, $\lambda_{\vartheta}(2S + 3S) - \lambda_{\vartheta}(1S) \sim 1$, seems to be almost impossible to reproduce, even resorting to extreme hypotheses for the polarizations of the $\chi_{bJ}(nP)$ states and their feed-down contributions to the production of the vector states (at least in the kinematical conditions of these low p_T measurements).

In the study reported in this paper we followed a cautious approach, fully developing the model by adapting the (only) free parameter to the J/ψ data, without trying to account for the Υ data at all, and then comparing the outcome of the computations to the Υ patterns. Only a posteriori we will discuss what one can infer from that comparison. Our reluctance in using the remarkable $\lambda_{\vartheta}(2S + 3S) - \lambda_{\vartheta}(1S) \sim 1$ difference as an *input* of our study is exclusively based on a principle of caution. Polarization measurements are always challenging and this case is even more demanding because the dimuon mass distribution reported by E866 suffers from a poor measurement resolution and a daunting signal-to-background ratio, so that the (unresolved) 2S and 3S states are not visible as a peak on the top of the underlying continuum. In contrast, the $\Upsilon(1S)$, $\Upsilon(2S)$ and $\Upsilon(3S)$ polarizations measured by CMS [9], in much more favourable experimental conditions, do not show any hint for differences between the three S-wave states. Clearly, if the patterns shown in Fig. 2 are not disturbed by experimental difficulties, their comparison to the CMS results points to the importance of the different experimental conditions: the collision energy, the longitudinal and transverse momentum ranges, and the use of a nuclear target (Cu) in the E866 data. In any case, it would certainly be very useful to have the fixed-target measurement repeated by another experiment, with improved detection capabilities.

3 Overall qualitative physical indications

The model presented in this paper, described in much more detail in the next section and then quantitatively tested in Section 5, can be very briefly summarised by saying that low p_T quarkonium production is dominated by two processes, the quarkonia produced in gluon-gluon fusion having longitudinal polarization and those produced in quark-antiquark annihilation having transverse polarization. The model is inspired by two qualitative physical observations revealed by a careful look at the J/ψ polarization patterns shown in the six panels of Fig. 1.

The first observation follows from the HERA-B measurements [41], which were performed considering in turn all three polarization frames and provide all three shape parameters, λ_{ϑ} , λ_{φ} and $\lambda_{\vartheta\varphi}$. As is already suggested by the global picture of J/ψ measurements (presented in Fig. 1) and can be more clearly and precisely seen in the top panels of Fig. 3, the magnitude of the polar anisotropy parameter λ_{ϑ} is systematically larger in the CS frame and smaller in the HX frame. At the same time, as shown in the bottom panels of Fig. 3, the azimuthal anisotropy parameter λ_{φ} increases in magnitude following the inverse hierarchy, being the largest in the HX frame and the smallest in the CS frame. It is important to appreciate that the differences between the values measured in the three frames *are* significant, contrary to what the displayed uncertainties could indicate at first sight, because the three sets of data points were obtained using exactly the same events and, hence, their uncertainties are strongly correlated. In other words, the *differences* between the three sets of parameters have much smaller uncertainties than those represented by the error bars, so that we can say that these differences are significantly larger than zero.

These two observed hierarchies reflect, to start with, the geometrical difference between the three frame definitions: the GJ polarization axis has always, for every p_T and x_F values,

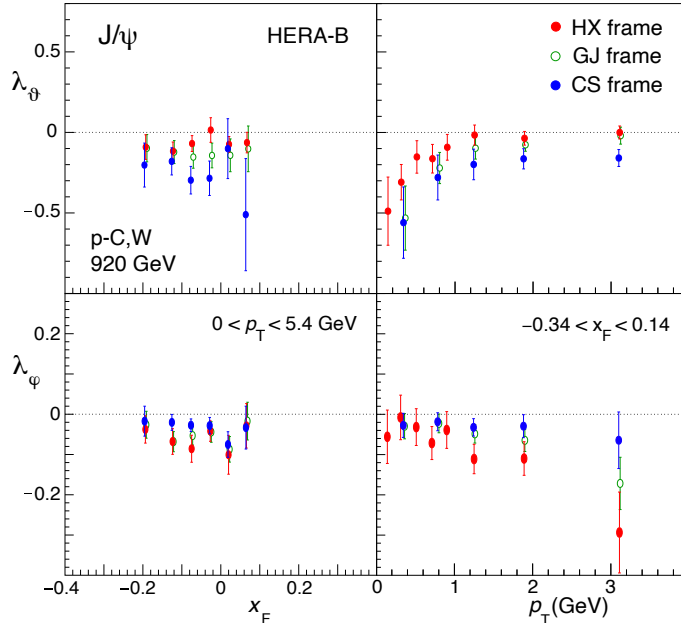


Figure 3: The J/ψ λ_θ and λ_ϕ parameters measured by HERA-B in the CS, GJ and HX frames, vs. x_F and p_T .

an intermediate direction between the CS and HX ones. On the other hand, and more importantly, the direction of the hierarchy, with the CS frame showing the largest polarization effect with the smallest azimuthal anisotropy, has one clear physical interpretation: the CS axis is the one that most naturally reflects the alignment of the J/ψ angular momentum. This provides relevant information regarding the topological nature of the involved processes: they must be, predominantly, of the 2-to-1 kind ($h_1 h_2 \rightarrow J/\psi$), where the produced object directly inherits the angular momentum state of the system of colliding partons, which is polarized along the direction of the collision. One can expect, a priori, that most of the mesons produced in 2-to-2 processes ($h_1 h_2 \rightarrow J/\psi + X$, where the J/ψ is emitted with a recoil hadron) have p_T much larger than the intrinsic momenta of the colliding partons, so that they have a negligible contribution to the low p_T yield with respect to the 2-to-1 processes. The observed polarization hierarchy further disfavours 2-to-2 contributions. In fact, in 2-to-2 processes the polarization legacy of the partons is shared between the two final objects and, while the angular momentum balance is more complex and depends on the coupling of the final states to the intermediate virtual particles, one can say that, in general, a natural alignment along the direction of the colliding partons is excluded.

An interesting illustration is provided by the case of the individual processes contributing to Drell–Yan production (DY) [49]. At the lowest order, DY production is a 2-to-1 process, characterized by a “natural” polarization along the collision direction, approximated by the CS axis. On the other hand, 2-to-2 processes (t - or s -channel) naturally lead to polarizations along the GJ and HX axes.

In the case of quarkonium production, the final state (the experimentally observable quarkonium state) evolves from an intermediate (singlet or octet) $Q\bar{Q}$ pre-resonance state, through the possible emission of one or more soft gluons. But the emission of one soft gluon (or more) in the bound state formation process does not qualify the process as “2-to-2”, given that we are talking about the process that produces the $Q\bar{Q}$ state: the emitted

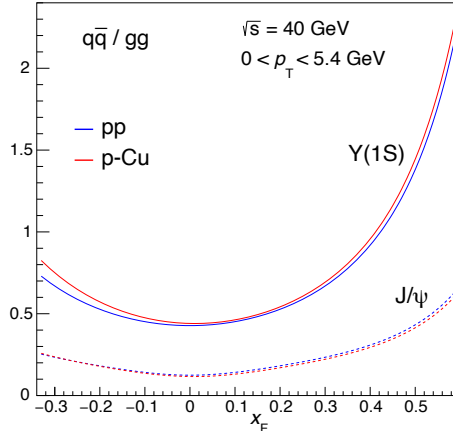


Figure 4: The $q\bar{q}$ to gg parton luminosity ratios for J/ψ and $\Upsilon(1S)$ production, vs. x_F , illustrated for conditions similar to those of the E866 and HERA-B experiments.

gluon is not to be seen as a final-state object of a 2-to-2 topology. Indeed, as long as the mass difference between the real final state and the virtual intermediate state is smaller than the total momentum ($\sqrt{(s/4)x_F^2 + p_T^2}$) of the observed state in the centre-of-mass of the colliding nucleons, the natural polarization direction of the final state coincides with the one of the intermediate state (that is, the direction of the colliding partons, in 2-to-1 processes) as discussed in Ref. [50] for the case of the radiative χ_c decays to J/ψ . These considerations motivate our assumption that the 2-to-1 $q\bar{q} \rightarrow Q\bar{Q}$ and $gg \rightarrow Q\bar{Q}$ scattering processes dominate, leading to strongly polarized quarkonia.

The second experimental indication is the observation of trends towards longitudinal J/ψ polarization at small $|x_F|$ (“mid-rapidity”). It is reasonable to suppose that this behaviour might be correlated with the relative dominance of gluon-gluon fusion at mid-rapidity, the $q\bar{q}$ annihilation process becoming more relevant as we move away from that central region. This hypothetical correlation can be better appreciated by looking at the ratio between the $q\bar{q}$ and the gg “luminosities”, both computed as the product of the corresponding parton distribution functions (PDFs). Figure 4 shows the x_F dependence of this $q\bar{q}/gg$ ratio, computed for $\sqrt{s} = 40$ GeV and for the J/ψ and $\Upsilon(1S)$ cases, using the CT14NLO [51] set of proton PDFs, as provided by the LHAPDF library [52]. The p-Cu curves were computed with the target PDFs (both for the protons and for the neutrons) modified to reflect nuclear effects, as provided by the EPPS16 package [53]. For the collision energies relevant for the E866 and HERA-B experiments, the nuclear effects on the PDFs play a negligible role. We clearly see that, as expected, the ratio has a minimum in the $x_F \sim 0$ region and increases as we move away from mid-rapidity.

It is also clear that the ratio is considerably higher for the $\Upsilon(1S)$ than for the J/ψ , reflecting the fact that, relatively speaking, $q\bar{q}$ annihilation becomes more important in the production of heavier particles. This is another important piece of evidence supporting the hypothesis that $q\bar{q}$ annihilation leads to transversely polarized quarkonia, given that, overall, the measurements collected in Figs. 1 and 2 indicate that the observed polarizations are more transverse for the Υ states than for the J/ψ .

This correlation between the measured quarkonium polarization patterns and the relative importance of the computed parton-parton luminosities is the central motivation of our postulate (to be further examined by confronting its implications with the existing mea-

surements) that gg fusion produces longitudinally polarized mesons while those produced through $q\bar{q}$ annihilation are transversely polarized. A physical justification supporting this assumption is beyond the scope of this paper, where we take a data-driven approach and let the measured patterns be our guiding principles. Nevertheless, it is not difficult to conceive that $q\bar{q}$ -induced J/ψ and Υ production might be analogous to the DY case and that, therefore, those quarkonia should be transversely polarized (angular momentum projection $J_z = \pm 1$) because of helicity conservation in the coupling between the annihilating quarks and a gluon. The longitudinal polarization of the quarkonia produced in gg fusion, on the other hand, may be justified, for example, with a dominating $J_z = 0$ projection of the gg system (then inherited by the $Q\bar{Q}$ state), which would be a necessary condition, forced by angular momentum conservation, if the scattering gluons were transversely polarized and formed a $J = 1$ state. Naturally, the CEM and NRQCD approaches are not expected to accommodate with the same proportion these two production channels (nor, more generally, any pair of oppositely-polarized processes), given the (in principle different) foreseen contributions of intermediate virtual $Q\bar{Q}$ states of different angular momentum quantum numbers. In fact, the scenario where gg fusion and $q\bar{q}$ annihilation produce quarkonia with maximally-different polarizations is the one most propitious for a test of the hadronization model.

The picture is made more complex, however, by the significant contribution of feed-down decays from P-wave states. Let us consider first the feed-down from an excited *vector* quarkonium. As long as mother and daughter have the same mechanism of production from partonic scattering, the feed-down decays from heavier vector states are “invisible” from the polarization point of view. This is confirmed by the observation that the J/ψ mesons produced in $\psi(2S) \rightarrow J/\psi \pi\pi$ decays have the same polarization as the $\psi(2S)$ mesons themselves [46] and by the analogous observation made in the Υ family [47,48]. On the contrary, P-wave states have, in general, different production mechanisms with respect to the vector states. Moreover, the χ_c and χ_b mesons decay to the J/ψ and Υ mesons with the emission of a transversely polarized photon, which alters the spin-alignment of the $Q\bar{Q}$ [50]. Therefore, we should expect that the J/ψ and Υ mesons produced in decays of P-wave states have different polarizations with respect to the directly produced ones. In particular, if large fractions of the observed vector quarkonia are produced through χ feed-down decays, we will probably observe a strong reduction of the transverse or longitudinal polarizations that could be measured if direct production were the dominating mechanism.

The J/ψ and Υ feed-down fractions from χ mesons depend on the experimental conditions: for example, they can be different if gg fusion or $q\bar{q}$ annihilation individually dominate, since different selection rules between the initial state and the final S- and P-wave states are expected in the two cases. We will consider a “central” scenario and two “extreme” ones, characterized by different values of the feed-down fractions; together, these scenarios should represent a reasonably conservative “uncertainty margin”, likely to cover the real values of these input variables in our model. Our central scenario assumes that the observed J/ψ sample is affected by a feed-down fraction from χ_c decays of around 19%, for both gg and $q\bar{q}$ production, corresponding to the central value of the HERA-B measurement [54]. The two extreme scenarios assume that the χ_c feed-down has a maximal impact on the observable prompt J/ψ polarization, as will be specified in the next section. Therefore, for these scenarios we use the larger value of 25%, representing an upper limit derived taking into account also the CDF [55] and LHCb [56] measurements. The feed-down fractions in the bottomonium family are not well known, especially in the low- p_T range relevant for the fixed-target results that we are addressing in this paper. On

the basis of LHCb measurements at forward rapidity [57] and of extrapolated trends of mid-rapidity LHC cross sections [58], we will assume that, for the central scenario, the $\Upsilon(1S)$ and $\Upsilon(2S+3S)$ results of E866 are affected by χ_b feed-down contributions of around 45% and 25%, respectively; for the two extreme scenarios we will use the respective upper limits of 60% and 50%.

Before concluding this section, it is important to note that our study is exclusively devoted to quarkonium production in the $x_F < 0.5$ domain and does not address the high x_F region, where a trend towards longitudinal polarization has been seen by E615 and E866 (in pion- and proton-nucleus collisions, respectively). Although certainly interesting in their own right [59, 60], this edge of phase space is likely to be dominated by processes that are not covered by the model that we discuss in this paper.

4 Description of the model

As anticipated in the previous section, our model is based on two main assumptions: 1) $Q\bar{Q}$ production is dominated by 2-to-1 topologies (qg contributions, producing at least one additional object besides the quarkonium, are, therefore, considered negligible); 2) the $gg \rightarrow Q\bar{Q}$ and $q\bar{q} \rightarrow Q\bar{Q}$ processes lead, respectively, to fully longitudinal and fully transverse polarizations of the *directly produced* J/ψ , $\psi(2S)$ and Υ mesons. For these “natural” polarizations we assume as quantization axis the (unobservable) relative direction of the colliding partons, which does not coincide (event-by-event) with the CS axis because of the (small but) nonzero parton transverse momenta, \vec{k}_{1T} and \vec{k}_{2T} .

In fact, for measurements performed at low p_T , small $|x_F|$ and light particles (the J/ψ in our case), the transverse component of the parton motion inside the colliding hadrons has an effect on the observable polarization. For the scope of the present discussion, the meaning of \vec{k}_T is extended with respect to the bare intrinsic momentum owned by partons for being confined inside a hadron of finite dimensions ($\Delta p \sim 1/(1 \text{ fm}) = 0.2 \text{ GeV}$), also considering other effects occurring during the scattering process and possibly influencing the direction of the partonic collision (soft gluon emissions, multiple scattering in the nuclear target, etc.). We will assume that, given these extra sources of transverse momentum kick, the parton k_T reaches a magnitude $\langle k_T^2 \rangle = \mathcal{O}(1 \text{ GeV}^2)$, compatible with the measured p_T distributions: $\langle p_T^2 \rangle \simeq 2 \langle k_T^2 \rangle \simeq 2 \text{ GeV}^2$ (see, e.g., Ref. [61]). The parton transverse momenta also provide the only source of quarkonium p_T considered in the model.

The vectors \vec{k}_{1T} and \vec{k}_{2T} are generated in space, with the two moduli following a Gaussian distribution of variance $\langle k_T^2 \rangle = 1 \text{ GeV}^2$ and the azimuthal angles ϕ_1 and ϕ_2 following uniform distributions. While the \vec{k}_T effect has a negligible influence for Υ production, it has a significant impact in the observable J/ψ polarization, as illustrated in Fig. 5 for fully transverse (solid lines) and fully longitudinal (dashed lines) natural polarizations, in the conditions of the HERA-B experiment but in a slightly larger (and positive) x_F range. The main effect (ignoring the slight p_T - and x_F -dependent modulations) is that the magnitude of the λ_ϑ parameter measured in the CS frame is reduced with respect to the values generated in the parton-parton frame, by about 20% and 10% for the fully transverse and fully longitudinal polarizations, respectively.

As expected, the CS frame remains the best approximation of the natural frame, because the λ_ϑ values observable in the GJ and HX frames depart more significantly from the natural one, an effect increasing with p_T . The λ_φ values seen in the three observation frames are also shown in Fig. 5, in the bottom panels, with the expected inverted hierarchy, similar to the one seen by HERA-B, as previously pointed out. There is a nonzero λ_φ

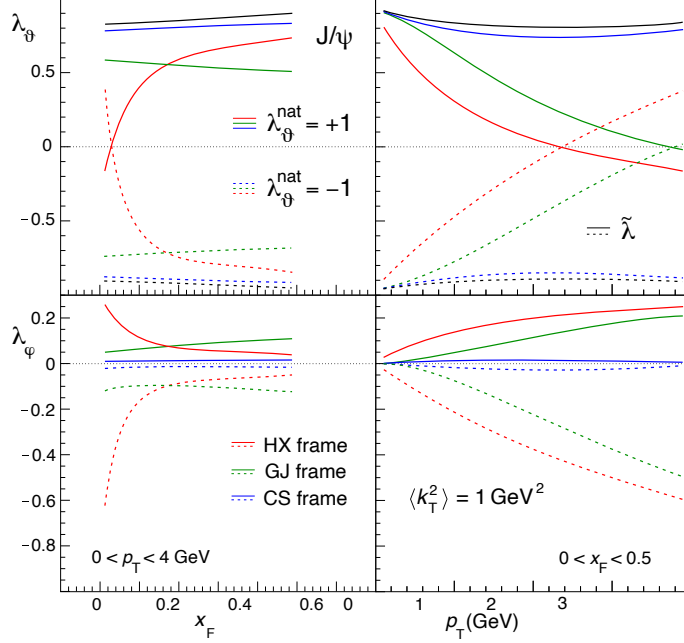


Figure 5: The parameters λ_ϑ and λ_φ as would be observed in the CS, GJ and HX frames for fully transverse and longitudinal J/ψ polarizations along the direction of the colliding partons, in the HERA-B experimental conditions, for $\langle k_T^2 \rangle = 1 \text{ GeV}^2$. The angular distribution parameters are shown as a function of x_F averaged over p_T (left) and vice versa (right). The invariant polarization parameter $\tilde{\lambda}$, shown in gray, is by definition identical in the three observation frames.

value also in the CS frame, as a result of the rotation from the natural frame. However, the transformation from the natural parton-parton to the “laboratory” CS frame is not a simple rotation in the production plane (around the y axis), as is the case between any two of the three experimental frames. While the magnitude of the polar anisotropy decreases exactly as in such ordinary frame rotations (for the same rotation angle), the correspondingly arising azimuthal anisotropy, $\lambda_\varphi \neq 0$, no longer geometrically compensates the $|\lambda_\vartheta^{\text{CS}}|$ decrease. In fact, in this case the rotation plane (formed by the parton-parton and proton-nucleon relative momentum directions) does not coincide with the experimentally defined production plane. The angle between the two planes changes from one event to the next, so that the azimuthal anisotropy resulting from the tilt between the natural polarization axis and the experimental axis tends to be smeared out in the integration over all events. Consequently, the invariant polarization parameter $\tilde{\lambda}$ [62, 63] (shown as gray curves on the top panels of Fig. 5), while slightly closer to the natural value, does not return its full magnitude: the natural polarization is unrecoverably smeared in any observation frame.

The relative proportion of quarkonia *directly* produced through $q\bar{q}$ annihilation and gg fusion processes and, therefore, their observable mixture of longitudinal and transverse polarizations, is fully determined in the model by the product of two ratios, R and r . The first one is the ratio between the $q\bar{q}$ and gg parton densities,

$$R = \frac{\sum_q [F_1^q(x_1, \hat{s}) F_2^{\bar{q}}(x_2, \hat{s}) + F_1^{\bar{q}}(x_1, \hat{s}) F_2^q(x_2, \hat{s})]}{F_1^g(x_1, \hat{s}) F_2^g(x_2, \hat{s})}, \quad (1)$$

where $\hat{s} = M_Q^2 + p_T^2$ and $x_1 x_2 = \hat{s}/s$, with M_Q being the quarkonium mass and $p_T = |\vec{k}_{1T} + \vec{k}_{2T}|$; the indexes 1 and 2 refer, respectively, to the beam proton and the target nucleon, and the sum is made over the participating quark flavours ($q = u, d$). Nuclear modification factors for the nucleon in the target, different for sea and valence quarks, are computed with the EPPS16 model [53] and applied in the definition of F_2 .

The second ratio is the one between the $q\bar{q}$ and gg partonic cross sections,

$$r = \frac{\hat{\sigma}(q\bar{q} \rightarrow \mathcal{Q})}{\hat{\sigma}(gg \rightarrow \mathcal{Q})}, \quad (2)$$

assumed to be universal, that is, identical for all considered vector quarkonia, $\mathcal{Q} = J/\psi, \psi(2S), \Upsilon(nS)$. In principle, one might be able to evaluate r within the context of specific model-dependent approaches, such as, for example, the NRQCD framework. It should be noted, however, that r is the ratio of the partonic cross sections, depending not only on the ‘‘short-distance parton-level cross sections’’ (the SDCs), which can be computed in perturbative QCD, but also on the probabilities of the transitions from the $Q\bar{Q}$ ‘‘pre-resonances’’ (singlet and octet states) into the final quarkonium state (the LDMEs). These probabilities represent non-perturbative evolution processes and are presently not calculated, but rather determined from global analyses of collider data. Besides, they are a priori different in the $q\bar{q}$ and gg cases, which, in general, produce pre-resonances of different angular momentum properties. In our study we deliberately try to remain as agnostic as possible regarding model-dependent inputs, so that we treat r as an empirical parameter, adjusted through the analysis of the J/ψ data.

The resulting natural polarization parameter λ (in the parton-parton CS frame), for a given mixture of $q\bar{q}$ and gg events (expressed by $R \times r$), is determined according to the sum rule presented in Eq. 11 of Ref. [29], reported here as a function of the $q\bar{q}$ and gg fractions, $f_{q\bar{q}} = R \times r / (1 + R \times r)$ and $f_{gg} = 1 / (1 + R \times r)$, and of the corresponding assumed polarizations, $\lambda^{q\bar{q}}$ and λ^{gg} :

$$\lambda = \frac{f_{q\bar{q}} \lambda^{q\bar{q}} / (3 + \lambda_\vartheta^{q\bar{q}}) + f_{gg} \lambda^{gg} / (3 + \lambda_\vartheta^{gg})}{f_{q\bar{q}} / (3 + \lambda_\vartheta^{q\bar{q}}) + f_{gg} / (3 + \lambda_\vartheta^{gg})} \quad (3)$$

This expression is explicitly x_F dependent because of the presence of R (that is, of the PDFs) in the $q\bar{q}$ and gg fractions, while a further kinematic dependence, also on p_T , is acquired by the polarization parameters when translated to the observable frames (CS and HX); this translation is performed by generating pseudo-events with a Monte Carlo method.

To turn the polarizations determined in this way, for the directly-produced quarkonium states, into values that can be compared with the measured data, we need to take into account the effect of the unknown feed-down contributions from the χ_c or χ_b states. We do so by considering three alternative scenarios, two of them representing extreme hypotheses. These scenarios have two kinds of ingredients: the natural λ_ϑ values for the J/ψ or Υ mesons produced in the decays of the χ_1 and χ_2 states, and the feed-down fractions from each of those states.

Concerning the polarizations, the central-value hypothesis corresponds to assuming that a) $q\bar{q}$ production leads to a (vector or P-wave) quarkonium state with angular momentum projection ± 1 , that is (besides the already mentioned $\lambda_\vartheta = +1$ for the directly produced vector quarkonia), $\lambda_\vartheta = -1/3$ for J/ψ or Υ mesons from χ_1 or χ_2 decays [50]; and that b) for gg production the assumed angular momentum projection is 0, meaning $\lambda_\vartheta = -1$,

+1 and $-3/5$, respectively for directly produced J/ψ or Υ mesons, and for those coming from χ_1 and χ_2 decays [50]. As variations of these hypotheses, defining the two alternative scenarios, we consider the extremes of the physical intervals for the polarizations of J/ψ or Υ mesons from χ_1 and χ_2 decays, $[-1/3, +1]$ and $[-3/5, +1]$, respectively. The scenarios using the most longitudinal and transverse χ polarizations are referred to by the labels “lower” and “upper”, respectively. For clarity, the natural polarizations assumed in the three scenarios are summarized in Table 2.

Table 2: Values of λ_ϑ considered in the generation of the J/ψ or Υ mesons resulting from feed-down decays of χ_1 or χ_2 mesons produced through gg fusion or $q\bar{q}$ annihilation, in the baseline “central” scenario and in two extreme scenarios, “lower” and “upper”, leading, respectively, to the most longitudinal and most transverse values for the natural polarization of the total prompt- J/ψ polarization. In all scenarios, the directly-produced vector states are generated with $\lambda_\vartheta = -1$ and $+1$ for gg fusion and $q\bar{q}$ annihilation, respectively.

		$\lambda_\vartheta^{\chi_1}$	$\lambda_\vartheta^{\chi_2}$
central	gg	+1	$-3/5$
	$q\bar{q}$	$-1/3$	$-1/3$
lower	$gg, q\bar{q}$	$-1/3$	$-3/5$
upper	$gg, q\bar{q}$	+1	+1

As already mentioned in the previous section, the small mass difference between the mother and daughter particles, in all considered cases, ensures that the natural angular momentum alignment direction is preserved in the decay [50]: also for indirect production we use, therefore, the parton-parton direction as quantization axis.

For the total χ feed-down fraction, $R_{\chi_1} + R_{\chi_2}$, we assume, as mentioned in the previous section, the values 19%, 45% and 25% for, respectively, the J/ψ , the $\Upsilon(1S)$ and the $\Upsilon(2S+3S)$ cases in the central scenario; the corresponding values in the extreme scenarios are 25%, 60% and 50%. We assume the ratio between the contributions of the two states to be $R_{\chi_1}/R_{\chi_2} = 1$ in the three scenarios, after verifying that its variation within the 0.6–1.4 range established by HERA-B [54] does not lead to significant changes in the results. Actually, the range of hypotheses assumed for the χ feed-down should be wide enough to cover possible dependences of the inputs on the experimental conditions, such as the x_F and p_T ranges of the different measurements.

5 Data vs. model for p-nucleus collisions

Figure 6 compares the HERA-B and E866 measurements of the J/ψ polarization parameters, as functions of x_F and p_T , with the corresponding curves computed with the model described in the previous section, using the central set of the CT14NLO [51] proton PDFs, properly adapting the calculations to the specific conditions (quarkonium state, collision energy, p_T and x_F coverage). The considered parameters are the λ_ϑ in the CS frame (where the model does not foresee visible deviations of λ_φ from zero, a prediction confirmed by the data, as seen in Fig. 3) and both λ_ϑ and λ_φ in the HX frame, where the two parameters share the magnitude of the natural polarization effect. For each of the three scenarios, a range of values for the only parameter not fixed by our hypotheses, the $q\bar{q}$ over gg cross

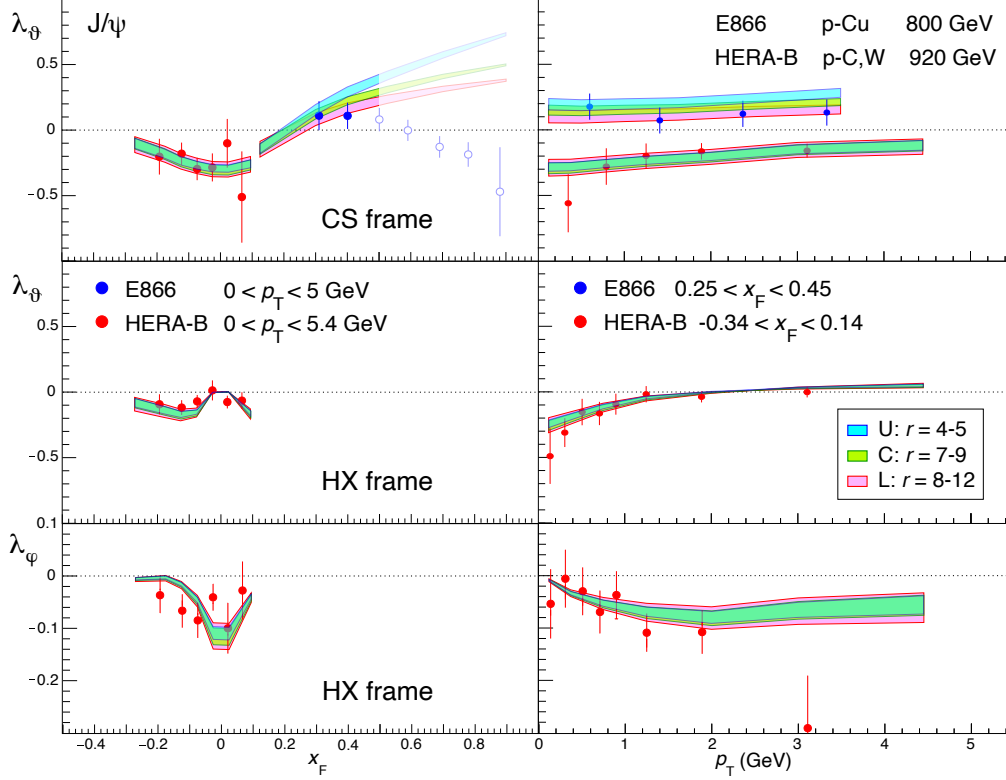


Figure 6: The x_F (left) and p_T (right) dependences of the J/ψ polarization parameters λ_ϑ in the CS (top) and HX (middle) frames, and λ_φ in the HX frame (bottom), as measured by HERA-B (red points) and E866 (blue points). The cyan, green and magenta bands represent, respectively, the upper (U), central (C) and lower (L) scenarios described in the text. Since our model is not expected to describe high- x_F quarkonium production, the E866 measurements for $x_F > 0.45$ are depicted as open circles.

section ratio, r , has been determined so as to maximize the agreement with the data within the $x_F \lesssim 0.5$ domain: the ranges are 4–5, 7–9 and 8–12, for the upper, central and lower scenarios, respectively.

The uncertainty in the χ_c feed-down contribution has a large effect on the numerical determination of r , but almost no influence on the agreement between model and data. The interesting outcome of this comparison is that it is *possible* to describe quite accurately the J/ψ data for $x_F \lesssim 0.5$, with the only substantial hypothesis that the directly produced vector quarkonium is transversely polarized along the relative direction of the colliding q and \bar{q} , and longitudinally polarized along that of the colliding gluons. This conclusion is reinforced by the comparison with the $\Upsilon(1S)$ E866 measurement (λ_ϑ in the CS frame), shown in Fig. 7 for the same r values as determined using the J/ψ data. The central scenario is in very good agreement with the data. It is true that the fourth p_T point departs from the band, by around three times its uncertainty, but the significance of this difference seems to be suspiciously overestimated when we consider that the λ_ϑ value measured for p_T values only around 1 GeV lower is perfectly reproduced by the model, and that almost no physical variations should be expected within such a small p_T interval, only one tenth of the particle mass.

The comparison considered until here involves 24 J/ψ and $\Upsilon(1S)$ data points measured

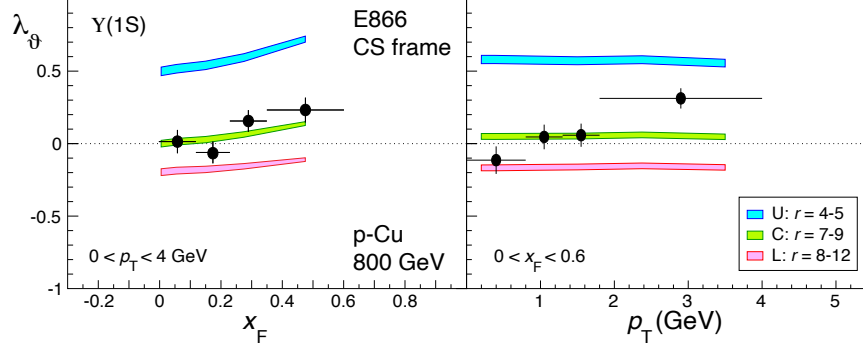


Figure 7: Same as Fig. 6, for the $\Upsilon(1S)$ λ_θ parameters, as measured by E866, in the CS frame.

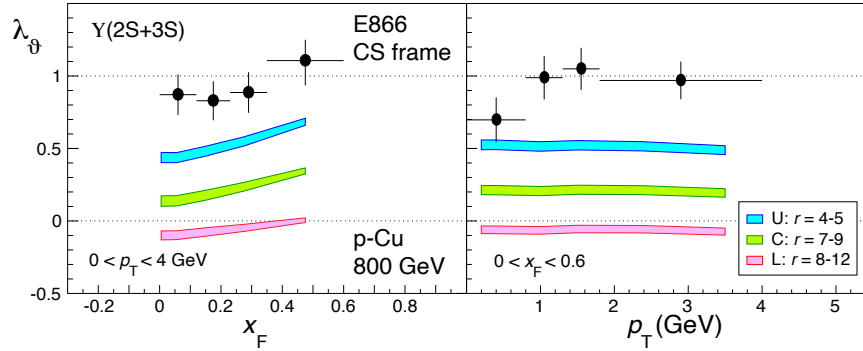


Figure 8: Same as Fig. 7, for the $\Upsilon(2S+3S)$.

as a function of x_F , plus 29 points vs. p_T . Only a couple of points have central values differing from the central-scenario curves by around two or three times their uncertainties. While it is true that not all of these measurements are statistically independent, this remains a remarkable outcome, especially given the simplicity of the model and the diversity of measured patterns. Therefore, we can state that the assumed interplay between $q\bar{q}$ and gg production, with their maximally different polarizations, describes the measured J/ψ and $\Upsilon(1S)$ polarizations, within a reasonable set of assumptions for the unknown χ polarizations: all four states, χ_{c1} , χ_{c2} , χ_{b1} and χ_{b2} , have angular momentum projections ± 1 and 0 , respectively along the $q\bar{q}$ and $g-g$ collision directions, just as assumed for the directly produced vector mesons. We remind that the χ feed-down fractions in the central scenario are fixed to the values 19% and 45%, respectively for the J/ψ and the $\Upsilon(1S)$, where the latter is only a reasonable guess, given the absence of suitable measurements. For this central scenario, the “universal” ratio between the $q\bar{q}$ and gg cross sections for quarkonium production is determined to be $r = 8 \pm 1$. The spread between the three bands (scenarios U, C and L) is much larger in Fig. 7 than in Fig. 6 because of the very uncertain χ_b feed-down fractions, mentioned before.

The last piece of our comparison concerns the E866 measurement for the (unresolved) $\Upsilon(2S)$ and $\Upsilon(3S)$ states, shown in Fig. 8: the data are significantly above all three model scenarios. This would seem to imply that the (slightly) heavier Υ states evade the “universality” of the assumed physical inputs in a rather drastic way. In fact, even if we assumed that the polarizations of the $\chi_b(2P)$ and $\chi_b(3P)$ states, contributing to the production of all

three $\Upsilon(nS)$ states, are extremely different from the polarizations of the $\chi_b(1P)$ states, only contributing to $\Upsilon(1S)$ production (certainly a rather unreasonable hypothesis), it would still be impossible to reproduce the data with our universal model for vector-quarkonium production: the only possibility would be to assume (possibly in addition) that the $q\bar{q}$ to gg cross section ratio is significantly higher for the only slightly heavier 2S and 3S states with respect to the 1S case, a hypothesis that would lead to a shift of all three bands towards the $\lambda_\vartheta = \pm 1$ limit.

However, as already mentioned before, these $\Upsilon(2S+3S)$ measurements are clearly a notable exception in the global panorama of the existing data. The first idea that comes to mind when seeing such a large discrepancy is to look for something that makes the $\Upsilon(2S+3S)$ measurement significantly different from the J/ψ and $\Upsilon(1S)$ measurements. After all, polarizations are notoriously difficult to measure and it could well be that the reported values are affected by experimental challenges. A first observation that can be made along those lines is that the J/ψ and $\Upsilon(1S)$ states are seen as very prominent peaks standing out of the underlying dimuon mass continuum, while the $\Upsilon(2S+3S)$ joint signal is not visible as a peak in the measured mass distribution (Fig. 1 of Ref. [42]), given the resolution and the signal-to-background ratio of the measurement. A second interesting observation is provided by the $\cos\vartheta$ distribution shown in Fig. 3-bottom of the E866 publication¹. The curve displayed in that figure, which corresponds to the fourth p_T bin, is distinctively asymmetric, thereby not corresponding to its legend (“ $1 + 0.98 \cos^2\vartheta$ ”) and, more importantly, clearly departing from the parity-conserving $1 + \lambda_\vartheta \cos^2\vartheta$ shape that must apply to the dimuons produced in decays of quarkonium states. We have fitted either the negative or the positive hemispheres of the reported $\cos\vartheta$ distribution and obtained λ_ϑ values that differ from each other by more than two times the published *total* uncertainties, an indication that those uncertainties might be underestimated. Nevertheless, the large discrepancies seen in Fig. 8 between the data points and the curves representing the central scenario would not disappear even if the $\Upsilon(2S+3S)$ λ_ϑ uncertainties would be increased by a factor of three. It would be very valuable to redo the analysis of the E866 data, this time using the $\Upsilon(2S+3S)$ over $\Upsilon(1S)$ ratio as a function of $\cos\vartheta$, which directly provides a measurement of the *difference* between the two polarizations, with smaller systematic uncertainties thanks to the cancellation of many potential effects in the ratio [64, 65]. Unfortunately, such a re-analysis is seemingly not possible [66], so that we will need to wait for future measurements to fully clarify this puzzle.

6 Data vs. model for pion-nucleus collisions

Using the r values determined from the proton-nucleus data (and the same three J/ψ feed-down scenarios in which the corresponding r ranges were determined), we will now see how the model compares with the J/ψ polarization measurements performed with pion beams.

Figure 9 shows the $q\bar{q}$ over gg parton luminosity ratios for J/ψ production, as computed using three different pion PDF sets: JAM21 [67], xFitter [68], and GRV-pi1 [69], obtained through the LHAPDF package [52]. The x_F dependence of this ratio, as well as its average value and the covered x_F range, depend quite significantly on the chosen PDF set, probably because of the poorly-known gluon density in the pion [27, 28]. In comparison, the differences between positive and negative pion beams are negligible. Also the nuclear

¹More precisely, in the figure of the arXiv version of the paper, given that the figure in the journal publication mistakenly shows the same distribution in the $\Upsilon(1S)$ and $\Upsilon(2S+3S)$ panels.

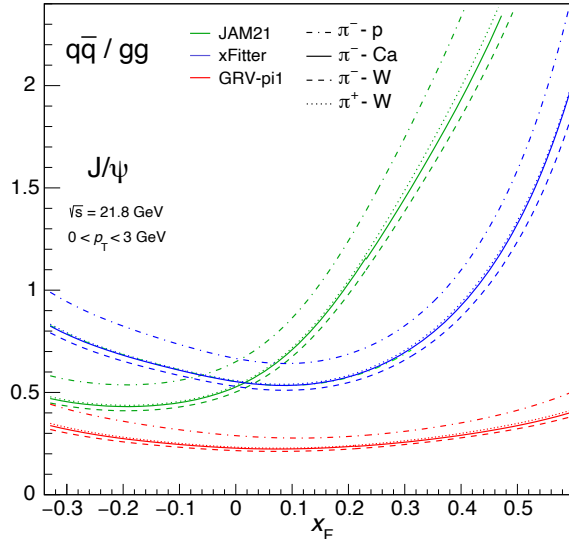


Figure 9: The $q\bar{q}$ over gg parton luminosity ratios, vs. x_F , for J/ψ production at the collision energy of E615 [34], for the JAM21, xFitter, and GRV-pi1 pion PDF sets, and for the π^- -p, π^- -Ca, π^- -W, and π^+ -W collision systems.

effects, computed using the EPPS16 model [53], have a minor impact, when we change the target from Ca to W, for example.

The dependence of the $q\bar{q}/gg$ ratio on the assumed PDF set directly translates into a corresponding variation in the polarization prediction, as seen in Fig. 10, where the several λ_θ vs. x_F and p_T bands are computed for π^- -W collisions at $\sqrt{s} = 21$ GeV, using the JAM21, xFitter and GRV-pi1 pion PDF sets. The filled bands represent the central scenario while the open ones represent the lower (solid lines) and upper (dashed lines) cases. We see that the E444 and E615 λ_θ measurements agree well with the model when the GRV-pi1 parton densities are used, and significantly depart from the bands representing the other two PDF sets. Figure 11 completes the data to model comparison, for pion-induced collisions, by showing the corresponding results for the E537 conditions, characterized by a lower collision energy, $\sqrt{s} = 15.3$ GeV, and a more backward x_F range, from 0 to 0.7.

We clearly see that accurate polarization measurements can provide precise constraints on global fits of pion PDFs, within the context of the rather general model discussed in this article (which, as previously mentioned, might only be valid in the $x_F \lesssim 0.5$ range).

7 Predictions for future measurements

New measurements in *proton*-induced collisions can strengthen our confidence in the basic model, where the observed polarization simply results from the interplay between $q\bar{q}$ and gg processes, and better tune its parameters. After this further step of model validation, improved *pion*-nucleus data can effectively represent a sensitive constraint on the pion PDFs. The AMBER experiment [70] at the CERN SPS accelerator, for example, is expected to collect large samples of J/ψ events using 190 GeV proton and pion beams, with carbon and tungsten targets. The top panel of Fig. 12 shows, for p-C collisions in the conditions of AMBER, the predicted x_F dependence of the J/ψ λ_θ parameter, in the CS frame, for the same three feed-down scenarios considered above. We do not show the λ_φ observable

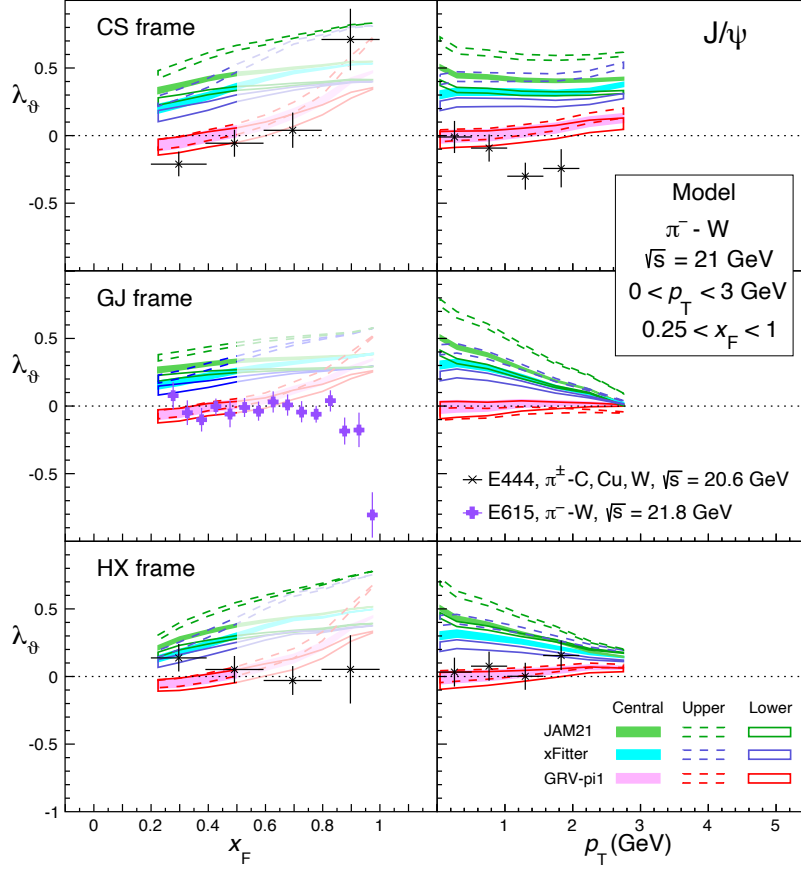


Figure 10: The x_F and p_T dependences of the J/ψ polarization parameter λ_ϑ , in the CS, GJ and HX frames, as measured by E444 and E615 in π -W collisions. The model predictions are computed using the JAM21, xFitter and GRV-pi1 pion PDF sets, for the three feed-down scenarios.

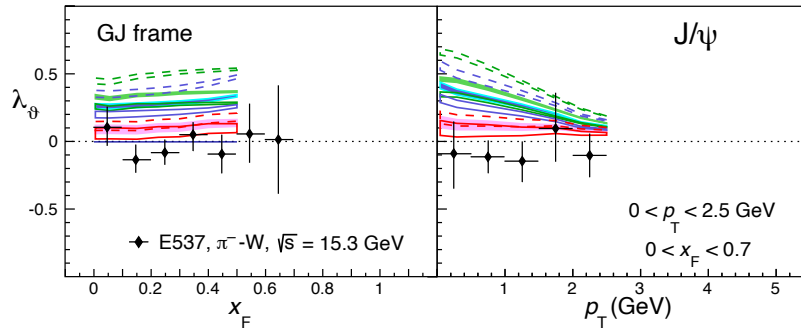


Figure 11: Same as Fig. 10, for the E537 conditions.

because, in this frame, it is perfectly compatible with being zero and flat with p_T ; correspondingly, the frame-independent parameter $\tilde{\lambda}$ [62,63] is essentially indistinguishable from λ_ϑ (and is, hence, also not shown).

The corresponding predictions for $\psi(2S)$ production are presented in the bottom panel. This measurement would be particularly interesting because it would test the model and

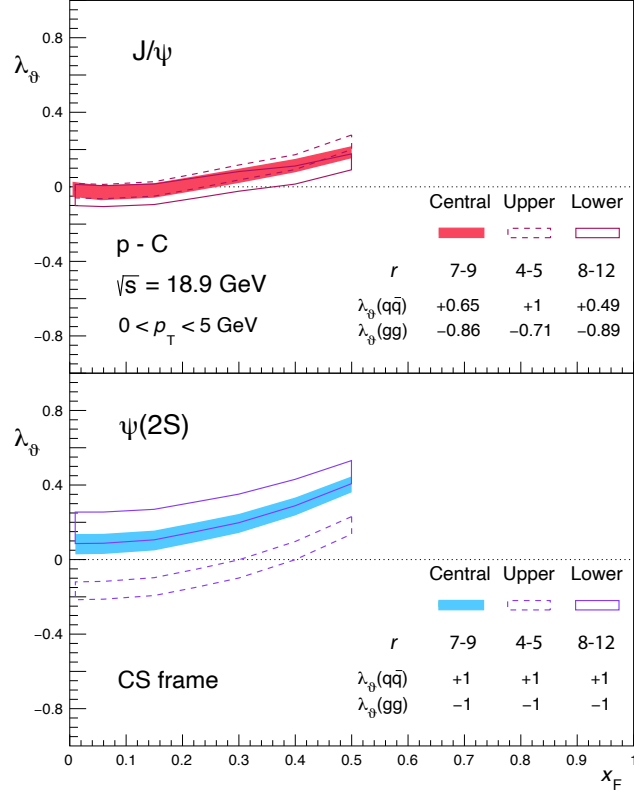


Figure 12: The x_F dependence of the λ_θ polarization parameter, in the CS frame, as predicted for J/ψ (top) and $\psi(2S)$ (bottom) production in p-C collisions at $\sqrt{s} = 18.9$ GeV (corresponding to the conditions of the AMBER experiment), for the three considered J/ψ feed-down scenarios.

constrain the pion PDFs in a cleaner and stronger way, free from the χ_c feed-down uncertainties: in this case, we simply have $\lambda_\theta = -1$ and $+1$ for gg fusion and $q\bar{q}$ annihilation, respectively, as for *direct* J/ψ production. The r range for $\psi(2S)$ production is assumed to be the same as for the J/ψ , indirectly depending, therefore, on the J/ψ feed-down scenario. This is why, in the figure, three sets of $\psi(2S)$ predictions are shown, despite the fact that $\psi(2S)$ production is intrinsically independent of feed-down.

The assumed equality of r for J/ψ and $\psi(2S)$ production follows the spirit of the factorization hypothesis motivating both the CEM and NRQCD models: we should, in fact, expect a cancellation of the long-distance bound-state formation effects, possibly differentiating $\psi(2S)$ and J/ψ , in the ratio of the $q\bar{q}/gg$ partonic cross sections (Eq. 2).

The comparison between the J/ψ and $\psi(2S)$ predictions shows that simultaneous measurements of both polarizations in proton-nucleus collisions can be used to fix the r range *and* determine the best J/ψ feed-down scenario, at the same time.

The corresponding J/ψ and $\psi(2S)$ predictions for pion-induced collisions are shown in Fig. 13. Here, the attention should be focused on the difference between the results obtained with the three PDF sets: the spread of polarization values, on average of order $\Delta\lambda_\theta \simeq 0.3$, shows that the measurement should be able to significantly discriminate between existing pion PDF sets or, alternatively, provide strong constraints on the future determination of new PDF sets.

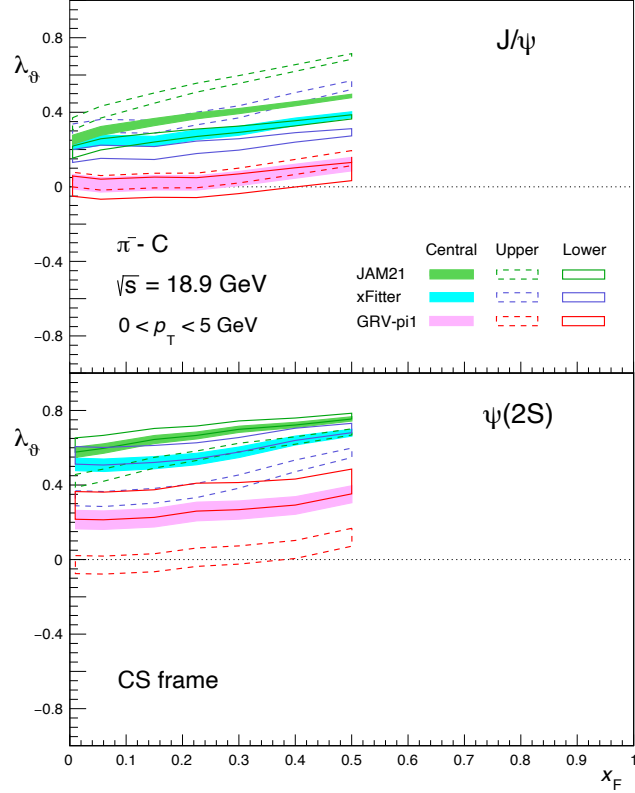


Figure 13: Same as Fig. 12, for π^- -C collisions. The bands represent the model predictions obtained in the three polarization scenarios, using the three pion PDF sets.

8 Summary

We proposed an interpretation of existing low- p_T quarkonium polarization measurements, performed in both proton-nucleus and pion-nucleus collisions, on the basis of a single and simple hypothesis: the production is dominated by 2-to-1 $q\bar{q}$ and gg processes, leading, respectively, to transversely and longitudinally polarized S-wave quarkonia, when directly produced. The feed-down from χ states is modelled through three hypotheses, reflecting the existing data, the central one being complemented by two extreme scenarios that, taken together, can be seen as representing the uncertainty that this input has on the results.

The J/ψ and $\Upsilon(1S)$ data are well reproduced by the model for $x_F \lesssim 0.5$; the trend to longitudinal polarization seen towards the high- x_F edge is a long-debated phenomenon that is not addressed in the present study. We have been unable to reproduce, even invoking barely reasonable variations in the feed-down contributions, the very large difference observed by E866 between the $\Upsilon(2S+3S)$ and $\Upsilon(1S)$ polarizations: an experimental problem, possibly related to the challenging discrimination of the $\Upsilon(2S+3S)$ signal from the background, might be the most reasonable explanation for this puzzling observation. More generally, some of the publications have not reported a complete evaluation of the uncertainties affecting the (sometimes rather old) measurements, which might explain the presence of suspicious fluctuations. It is clear that improved measurements are needed for a better understanding of the picture of quarkonium production at low p_T .

The calculations made for the comparisons with the pion-nucleus data reveal an interesting correlation between the J/ψ polarization and the assumed parton densities: the

predicted polarization depends on the adopted PDF set much more than on any other model input, directly reflecting the large variation of the $q\bar{q}/gg$ parton luminosity ratio, for which the three considered sets differ by a factor of 2 or more, with a strong dependence on x_F and p_T . While the GRV set reproduces reasonably well the existing data, the uncertainty represented by the differences between the three sets clearly indicates that the polarization observable has the potential to provide a strong constraint on the pion PDFs. With this motivation, we reported predictions for AMBER, as an example of an experiment capable of performing a further validation of our simple model, through improved J/ψ (“calibration”) measurements in proton-nucleus collisions, and, subsequently, constrain the pion PDFs with corresponding measurements in pion-nucleus collisions. We also emphasized the important role that a measurement of the $\psi(2S)$ polarization can have, by virtue of its independence from hypotheses on the χ_c feed-down contributions, both to validate the model and to determine the pion PDFs.

P.F. and C.L. acknowledge support from Fundação para a Ciência e a Tecnologia, Portugal, under contract CERN/FIS-PAR/0010/2019

References

- [1] N. Brambilla et al. *Eur. Phys. J. C* **71** (2011) 1534, doi:10.1140/epjc/s10052-010-1534-9, arXiv:1010.5827.
- [2] G. Bodwin, E. Braaten, and P. Lepage *Phys. Rev. D* **51** (1995) 1125, doi:10.1103/PhysRevD.51.1125, arXiv:hep-ph/9407339. [Erratum: *Phys. Rev. D* 55, 5853 (1997)].
- [3] R. Baier and R. Rückl *Phys. Lett. B* **102** (1981) 364, doi:10.1016/0370-2693(81)90636-5.
- [4] J.-P. Lansberg *Eur. Phys. J. C* **61** (2009) 693, doi:10.1140/epjc/s10052-008-0826-9, arXiv:0811.4005.
- [5] V. D. Barger, W.-Y. Keung, and R. J. N. Phillips *Phys. Lett. B* **91** (1980) 253, doi:10.1016/0370-2693(80)90444-X.
- [6] V. D. Barger, W.-Y. Keung, and R. J. N. Phillips *Z. Phys. C* **6** (1980) 169, doi:10.1007/BF01588844.
- [7] CDF Coll. *Phys. Rev. Lett.* **108** (2012) 151802, doi:10.1103/PhysRevLett.108.151802, arXiv:1112.1591.
- [8] CMS Coll. *Phys. Lett. B* **727** (2013) 381, doi:10.1016/j.physletb.2013.10.055, arXiv:1307.6070.
- [9] CMS Coll. *Phys. Rev. Lett.* **110** (2013) 081802, doi:10.1103/PhysRevLett.110.081802, arXiv:1209.2922.
- [10] LHCb Coll. *Eur. Phys. J. C* **73** (2013) 2631, doi:10.1140/epjc/s10052-013-2631-3, arXiv:1307.6379.
- [11] LHCb Coll. *Eur. Phys. J. C* **74** (2014) 2872, doi:10.1140/epjc/s10052-014-2872-9, arXiv:1403.1339.

- [12] LHCb Coll. *JHEP* **12** (2017) 110, doi:10.1007/JHEP12(2017)110, arXiv:1709.01301.
- [13] M. Butenschön and B. A. Kniehl *Phys. Rev. Lett.* **108** (2012) 172002, doi:10.1103/PhysRevLett.108.172002, arXiv:1201.1872.
- [14] K.-T. Chao et al. *Phys. Rev. Lett.* **108** (2012) 242004, doi:10.1103/PhysRevLett.108.242004, arXiv:1201.2675.
- [15] B. Gong, L.-P. Wan, J.-X. Wang, and H.-F. Zhang *Phys. Rev. Lett.* **110** (2013) 042002, doi:10.1103/PhysRevLett.110.042002, arXiv:1205.6682.
- [16] M. Butenschön and B. A. Kniehl *Mod. Phys. Lett. A* **28** (2013) 1350027, doi:10.1142/S0217732313500272, arXiv:1212.2037.
- [17] P. Faccioli et al. *Phys. Lett. B* **736** (2014) 98, doi:10.1016/j.physletb.2014.07.006, arXiv:1403.3970.
- [18] G. T. Bodwin et al. *Phys. Rev. D* **93** (2016) 034041, doi:10.1103/PhysRevD.93.034041, arXiv:1509.07904.
- [19] P. Faccioli et al. *Eur. Phys. J. C* **78** (2018) 268, doi:10.1140/epjc/s10052-018-5755-7, arXiv:1802.01106.
- [20] P. Faccioli and C. Lourenço *Eur. Phys. J. C* **79** (2019) 457, doi:10.1140/epjc/s10052-019-6968-0, arXiv:1905.09553.
- [21] V. Cheung and R. Vogt *Phys. Rev. D* **104** (2021) 094026, doi:10.1103/PhysRevD.104.094026, arXiv:2102.09118.
- [22] S. P. Baranov, A. V. Lipatov, and N. P. Zotov *Eur. Phys. J. C* **75** (2015) 455, doi:10.1140/epjc/s10052-015-3689-x, arXiv:1508.05480.
- [23] S. P. Baranov, A. V. Lipatov, and N. P. Zotov *Phys. Rev. D* **93** (2016) 094012, doi:10.1103/PhysRevD.93.094012, arXiv:1510.02411.
- [24] Y.-Q. Ma and R. Vogt *Phys. Rev. D* **94** (2016) 114029, doi:10.1103/PhysRevD.94.114029, arXiv:1609.06042.
- [25] V. Cheung and R. Vogt *Phys. Rev. D* **98** (2018) 114029, doi:10.1103/PhysRevD.98.114029, arXiv:1808.02909.
- [26] V. Cheung and R. Vogt *Phys. Rev. D* **99** (2019) 034007, doi:10.1103/PhysRevD.99.034007, arXiv:1811.11570.
- [27] W.-C. Chang, J.-C. Peng, S. Platchkov, and T. Sawada *Phys. Rev. D* **102** (2020) 054024, doi:10.1103/PhysRevD.102.054024, arXiv:2006.06947.
- [28] C.-Y. Hsieh et al. *Chin. J. Phys.* **73** (2021) 1510, doi:10.1016/j.cjph.2021.06.001, arXiv:2103.11660.
- [29] P. Faccioli, C. Lourenço, J. Seixas, and H. Wöhri *Eur. Phys. J. C* **69** (2010) 657, doi:10.1140/epjc/s10052-010-1420-5, arXiv:1006.2738.
- [30] E537 Coll. *Phys. Rev. D* **48** (1993) 5067, doi:10.1103/PhysRevD.48.5067.

- [31] WA11 Coll. *Phys. Lett. B* **82** (1979) 145, doi:10.1016/0370-2693(79)90446-5.
- [32] NA60 Coll. *Eur. Phys. J. C* **43** (2005) 167, doi:10.1140/epjc/s2005-02208-y.
- [33] E444 Coll. *Phys. Rev. Lett.* **43** (1979) 1219, doi:10.1103/PhysRevLett.43.1219.
- [34] E615 Coll. *Phys. Rev. Lett.* **58** (1987) 2523, doi:10.1103/PhysRevLett.58.2523.
- [35] NA3 Coll. *Z. Phys. C* **20** (1983) 101, doi:10.1007/BF01573213.
- [36] WA92 Coll. *Nucl. Phys. B* **557** (1999) 3, doi:10.1016/S0550-3213(99)00412-5.
- [37] E672/E706 Coll. *Phys. Rev. D* **53** (1996) 4723, doi:10.1103/PhysRevD.53.4723.
- [38] E672/E706 Coll. *Phys. Rev. D* **62** (2000) 012001, doi:10.1103/PhysRevD.62.012001, arXiv:hep-ex/9910005.
- [39] E771 Coll. *Phys. Rev. D* **55** (1997) 3927, doi:10.1103/PhysRevD.55.3927.
- [40] E866 Coll. *Phys. Rev. Lett.* **91** (2003) 211801, doi:10.1103/PhysRevLett.91.211801, arXiv:hep-ex/0308001.
- [41] HERA-B Coll. *Eur. Phys. J. C* **60** (2009) 517, doi:10.1140/epjc/s10052-009-0957-7, arXiv:0901.1015.
- [42] E866 Coll. *Phys. Rev. Lett.* **86** (2001) 2529, doi:10.1103/PhysRevLett.86.2529, arXiv:hep-ex/0011030.
- [43] J. C. Collins and D. E. Soper *Phys. Rev. D* **16** (1977) 2219, doi:10.1103/PhysRevD.16.2219.
- [44] K. Gottfried and J. D. Jackson *Nuovo Cim.* **33** (1964) 309, doi:10.1007/BF02750195.
- [45] P. Faccioli *Mod. Phys. Lett. A* **27** (2012) 1230022, doi:10.1142/S0217732312300224, arXiv:1207.2050.
- [46] BES Coll. *Phys. Rev. D* **62** (2000) 032002, doi:10.1103/PhysRevD.62.032002, arXiv:hep-ex/9909038.
- [47] CLEO Coll. *Phys. Rev. D* **30** (1984) 1433, doi:10.1103/PhysRevD.30.1433.
- [48] CLEO Coll. *Phys. Rev. D* **58** (1998) 052004, doi:10.1103/PhysRevD.58.052004, arXiv:hep-ex/9802024.
- [49] P. Faccioli, C. Lourenço, J. Seixas, and H. K. Wöhri *Phys. Rev. D* **83** (2011) 056008, doi:10.1103/PhysRevD.83.056008, arXiv:1102.3946.
- [50] P. Faccioli, C. Lourenço, J. Seixas, and H. K. Wöhri *Phys. Rev. D* **83** (2011) 096001, doi:10.1103/PhysRevD.83.096001, arXiv:1103.4882.
- [51] S. Dulat et al. *Phys. Rev. D* **93** (2016) 033006, doi:10.1103/PhysRevD.93.033006, arXiv:1506.07443.
- [52] A. Buckley et al. *Eur. Phys. J. C* **75** (2015) 132, doi:10.1140/epjc/s10052-015-3318-8, arXiv:1412.7420.

- [53] K. J. Eskola, P. Paakkinen, H. Paukkunen, and C. A. Salgado *Eur. Phys. J. C* **77** (2017) 163, doi:10.1140/epjc/s10052-017-4725-9, arXiv:1612.05741.
- [54] HERA-B Coll. *Phys. Rev. D* **79** (2009) 012001, doi:10.1103/PhysRevD.79.012001, arXiv:0807.2167.
- [55] CDF Coll. *Phys. Rev. Lett.* **98** (2007) 232001, doi:10.1103/PhysRevLett.98.232001, arXiv:hep-ex/0703028.
- [56] LHCb Coll. *Phys. Lett. B* **718** (2012) 431, doi:10.1016/j.physletb.2012.10.068, arXiv:1204.1462.
- [57] LHCb Coll. *Eur. Phys. J. C* **74** (2014) 3092, doi:10.1140/epjc/s10052-014-3092-z, arXiv:1407.7734.
- [58] P. Faccioli, C. Lourenço, M. Araújo, and J. Seixas *Eur. Phys. J. C* **78** (2018) 118, doi:10.1140/epjc/s10052-018-5610-x, arXiv:1802.01102.
- [59] E. L. Berger and S. J. Brodsky *Phys. Rev. Lett.* **42** (1979) 940, doi:10.1103/PhysRevLett.42.940.
- [60] E. L. Berger *Z. Phys. C* **4** (1980) 289, doi:10.1007/BF01421570.
- [61] HERA-B Coll. *Eur. Phys. J. C* **60** (2009) 525, doi:10.1140/epjc/s10052-009-0965-7, arXiv:0812.0734.
- [62] P. Faccioli, C. Lourenço, and J. Seixas *Phys. Rev. Lett.* **105** (2010) 061601, doi:10.1103/PhysRevLett.105.061601, arXiv:1005.2601.
- [63] P. Faccioli, C. Lourenço, and J. Seixas *Phys. Rev. D* **81** (2010) 111502(R), doi:10.1103/PhysRevD.81.111502, arXiv:1005.2855.
- [64] CMS Coll. *Phys. Rev. Lett.* **124** (2020) 162002, doi:10.1103/PhysRevLett.124.162002, arXiv:1912.07706.
- [65] P. Faccioli, C. Lourenço, and T. Madlener *Eur. Phys. J. C* **80** (2020) 623, doi:10.1140/epjc/s10052-020-8201-6, arXiv:2006.15446.
- [66] M. Leitch (spokesperson of the E866 collaboration), private communication.
- [67] P. C. Barry, N. Sato, W. Melnitchouk, and C.-R. Ji *Phys. Rev. Lett.* **121** (2018) 152001, doi:10.1103/PhysRevLett.121.152001, arXiv:1804.01965.
- [68] I. Novikov et al. *Phys. Rev. D* **102** (2020) 014040, doi:10.1103/PhysRevD.102.014040, arXiv:2002.02902.
- [69] M. Gluck, E. Reya, and A. Vogt *Z. Phys. C* **53** (1992) 651, doi:10.1007/BF01559743.
- [70] AMBER Coll. *Few Body Syst.* **63** (2022) 72, doi:10.1007/s00601-022-01769-7.